# Supplementary Figures and Tables

## Article Title:

# Multiparameter mobile blood analysis for complete blood count utilizing contrast-enhanced defocusing imaging and machine vision

Duan Chen,[a,b] Ning Li,[a,b] Shaoqun Zeng,[a,b] Xiaohua Lv,[a,b] Li Chen,[c] Xiuli Liu,[a,b*], and Qinglei Hu,[a,b*]

**Supplementary Figures**

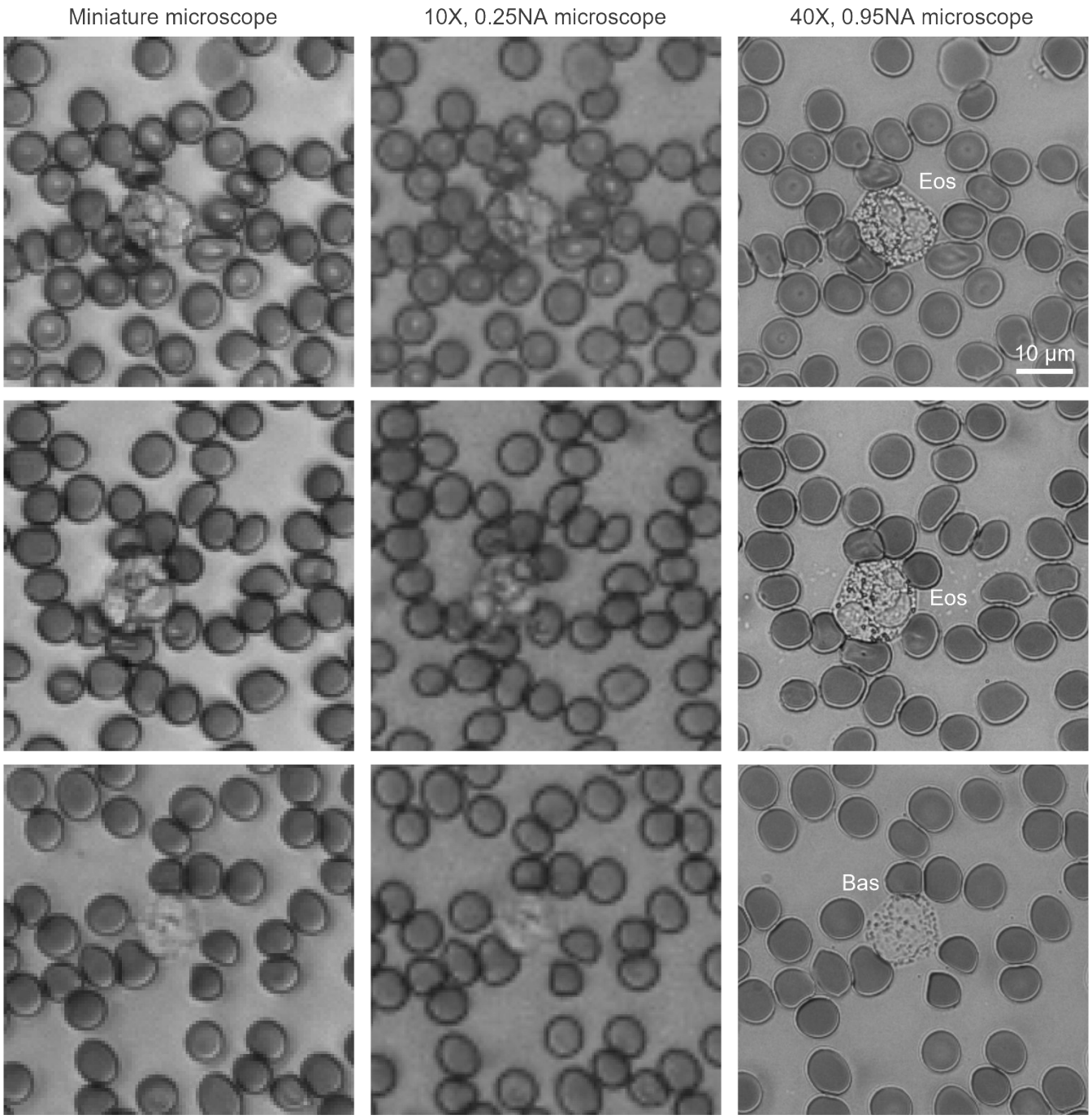


Fig. 1 CEDI images, without up-sampling, captured by the miniature microscope, 10X, 0.25NA microscope, and the 40X, 0.95NA microscope, respectively. Eos: eosinophil; Bas: basophil.

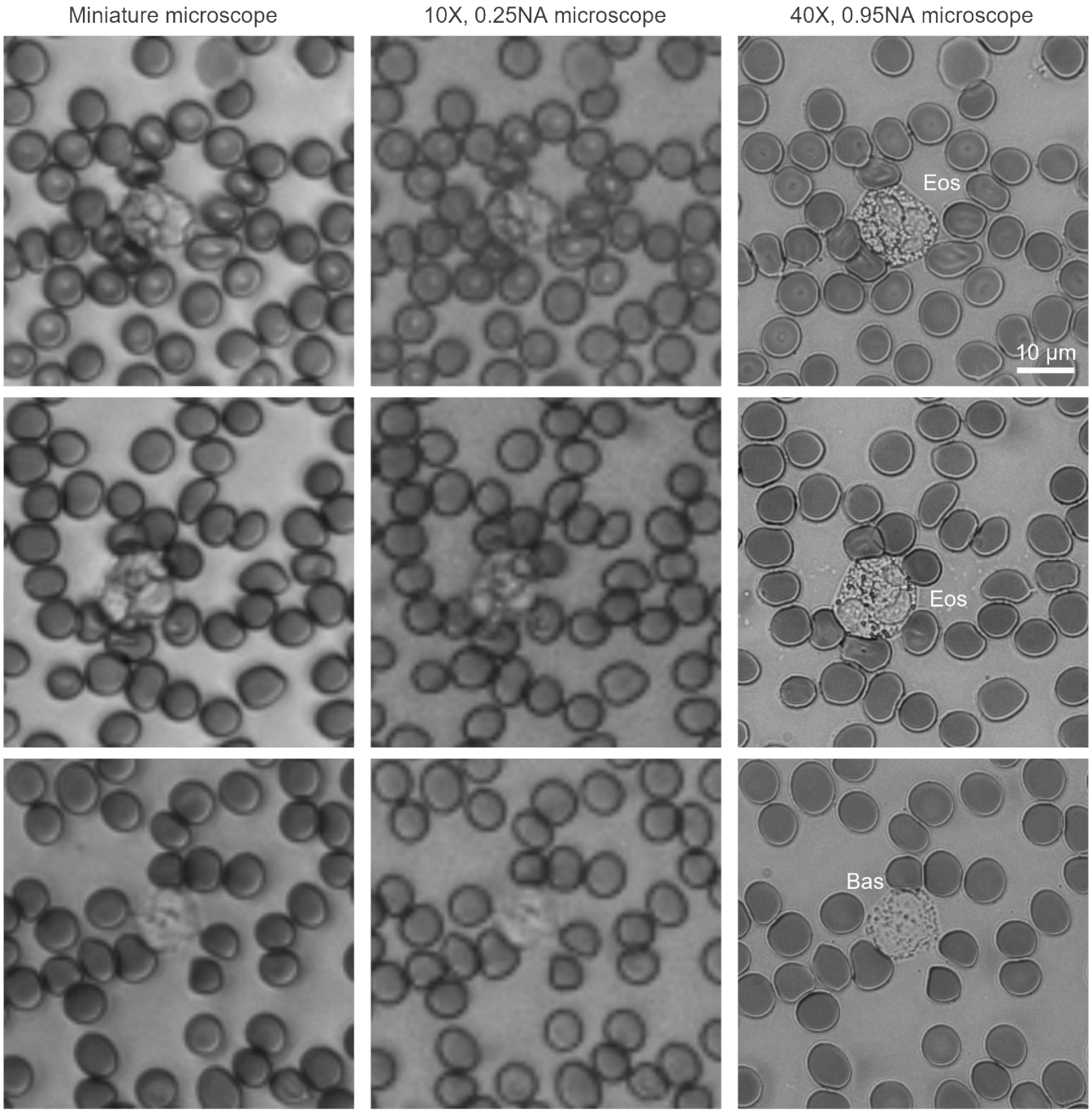


Fig. 2 CEDI images, with up-sampling, captured by the miniature microscope, 10X, 0.25NA microscope, and the 40X, 0.95NA microscope, respectively. Eos: eosinophil; Bas: basophil.

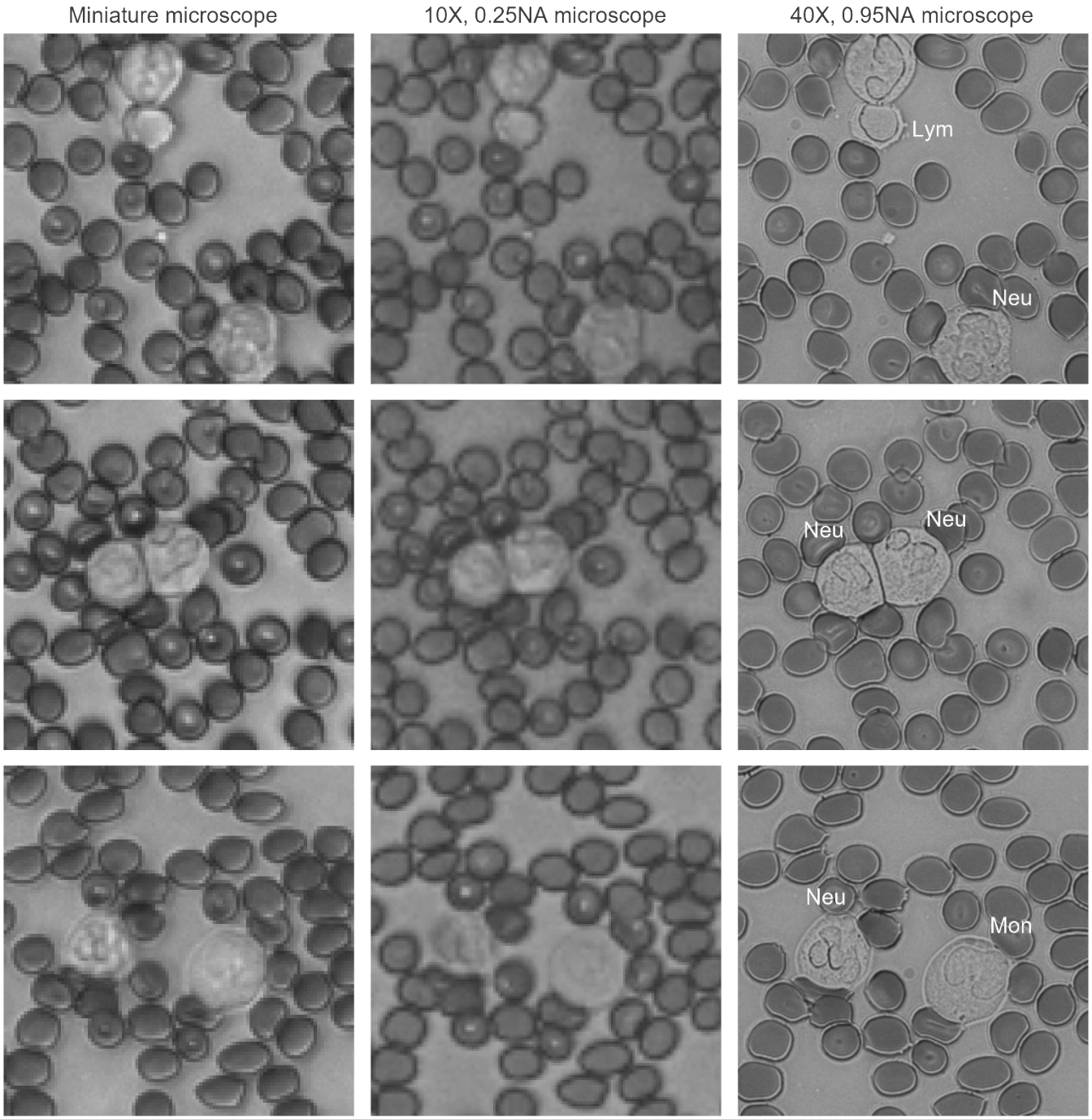


Fig. 3 CEDI images, without up-sampling, captured by the miniature microscope, 10X, 0.25NA microscope, and the 40X, 0.95NA microscope, respectively. Neu: neutrophil; Lym: lymphocyte; Mon: monocyte.

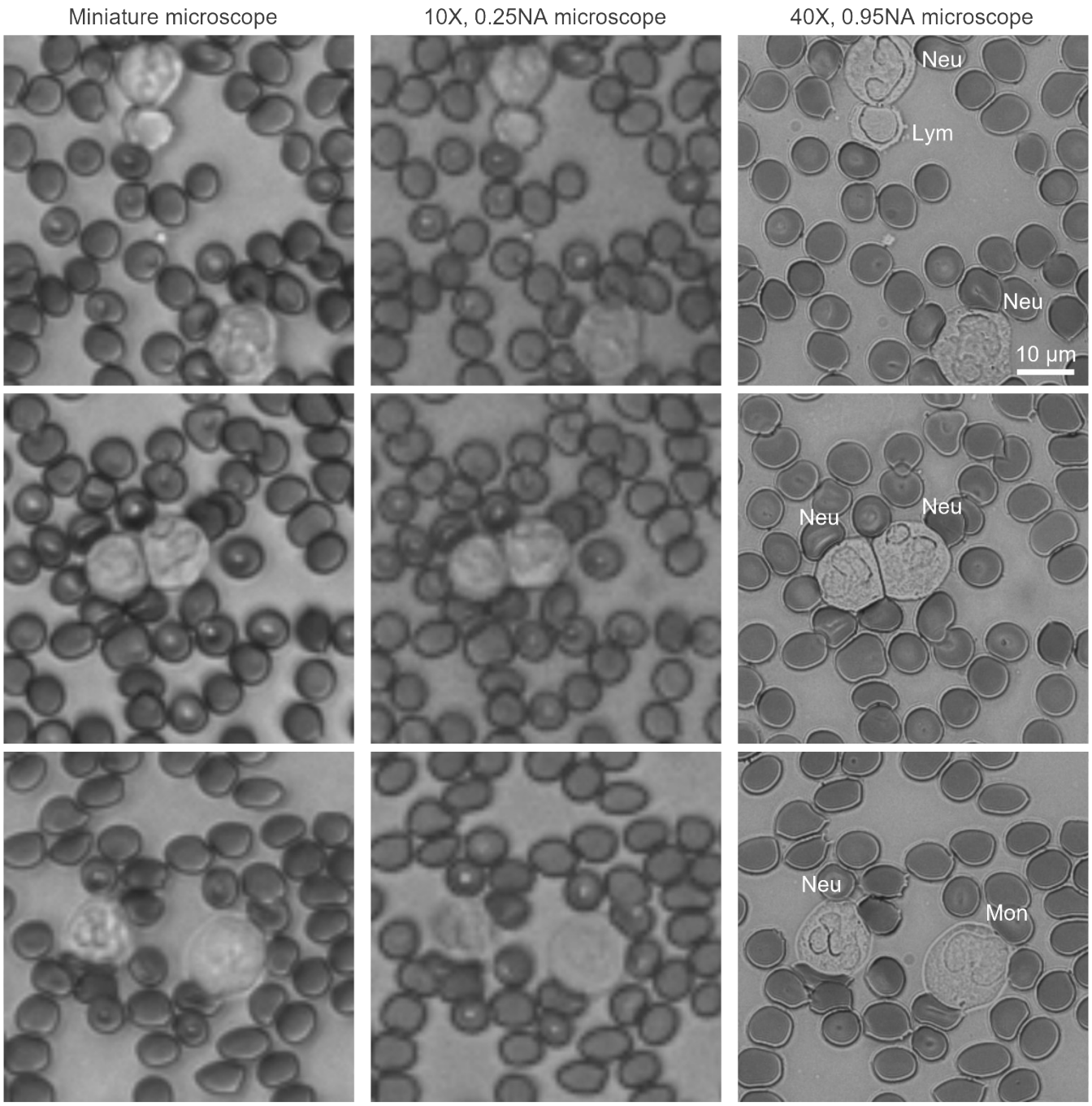


Fig. 4 CEDI images, with up-sampling, captured by the miniature microscope, 10X, 0.25NA microscope, and the 40X, 0.95NA microscope, respectively. Neu: neutrophil; Lym: lymphocyte; Mon: monocyte.

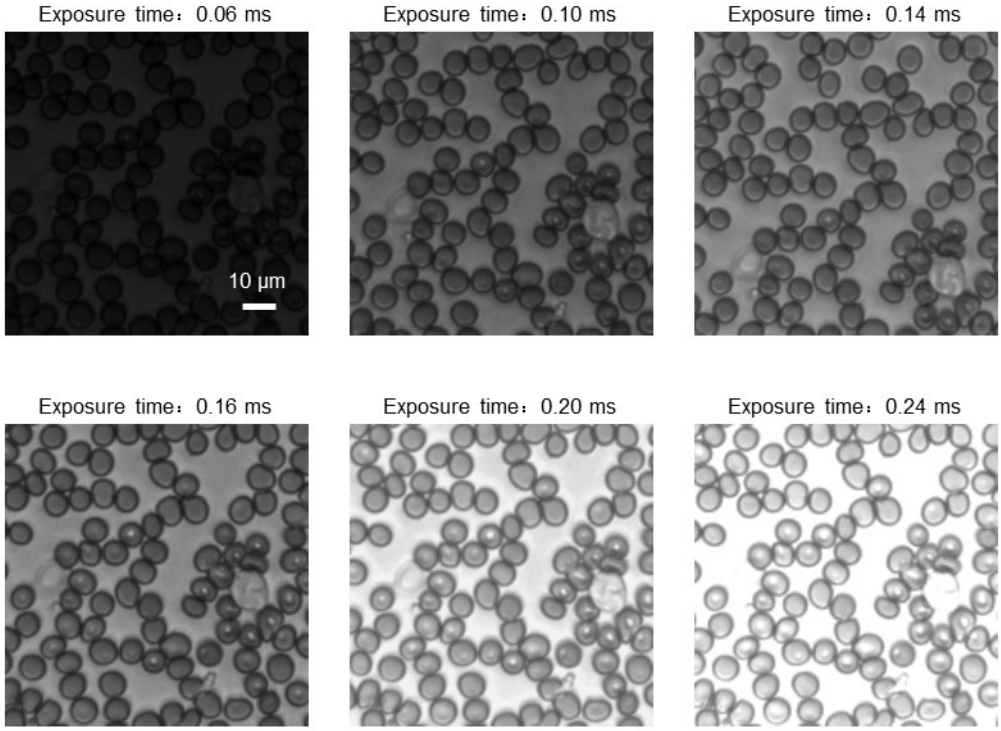


Fig. 5 Some CEDI images with different exposure times.

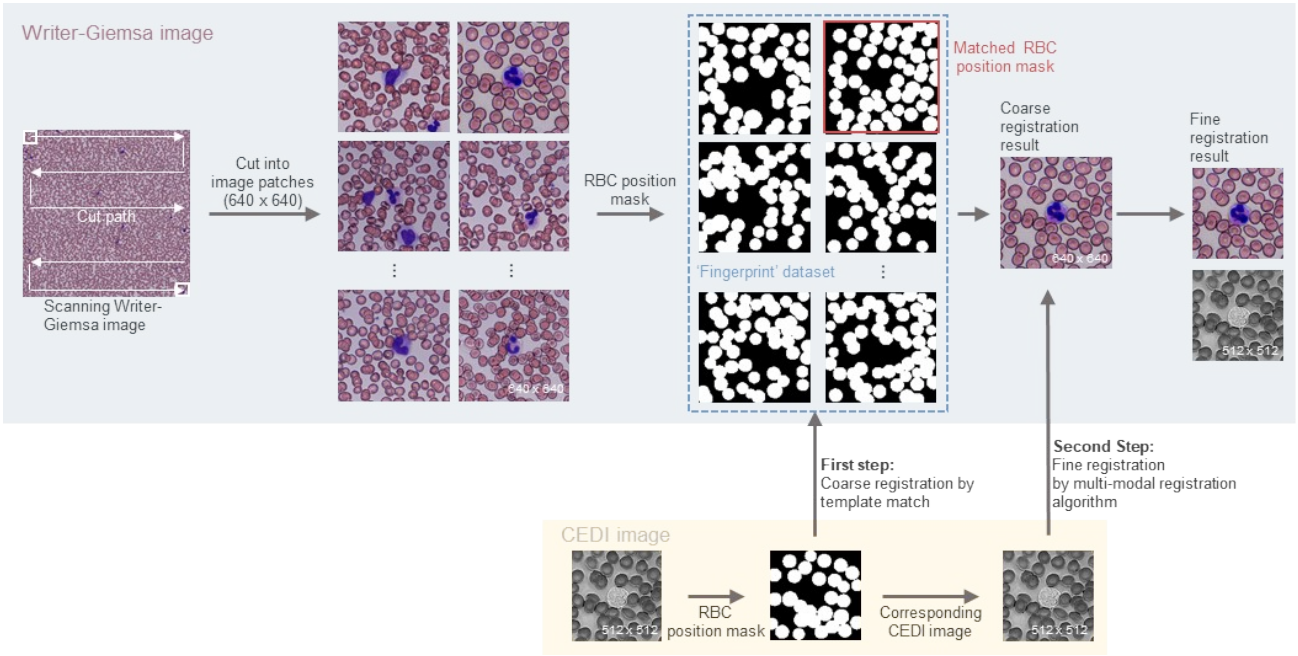


Fig. 6 The two-step image registration algorithm for the CEDI images by the miniature microscope and the Wright-Giemsa images. The RBC position mask images (binary images generated after performing the RBC segmentation algorithm) were adopted as the 'fingerprint' characteristics of the CEDI images and the Wright-Giemsa images. In the image preprocessing stage, the Wright-Giemsa images were cut into small image patches with image sizes of 640 x 640, following a cut path of the 'z' shape. Then the RBC segmentation algorithm introduced in the main text was performed to obtain the RBC position mask images of all the image patches ('fingerprint' dataset of the Wright-Giemsa images). The RBC position mask of the input CEDI image (image size of 512 x 512) would also be obtained by the RBC segmentation algorithm. After the image preprocessing, the two-step registration algorithm containing coarse and fine registration steps would be performed. The matched RBC position mask from the 'fingerprint' dataset for the RBC position mask image of the input CEDI image was searched by the coarse registration algorithm based on template matching, with a similarity criterion of minimum absolute difference (MAD). The fine registration algorithm based on the multimodal registration from MATLAB was used to correct the affine transformation between the Writer-Giemsa image (coarse registration result according to the matched RBC position mask) and the magnified CEDI image. Finally, the matched Wrigher-Giemsa and CEDI images with image sizes of 512x512 were obtained.

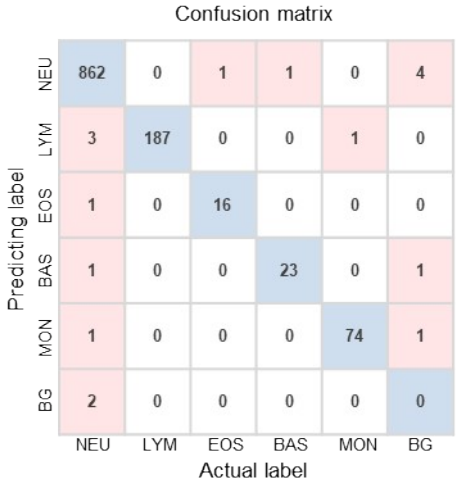


Fig. 7 Confusion matrix. The horizontal axis presents the actual number of instances, and the vertical axis shows the predicted number of instances from the trained network. NEU: Neutrophil, LYM: Lymphocyte, EOS: Eosinophil, BAS: Basophil, MON: Monocyte, BG: Background.

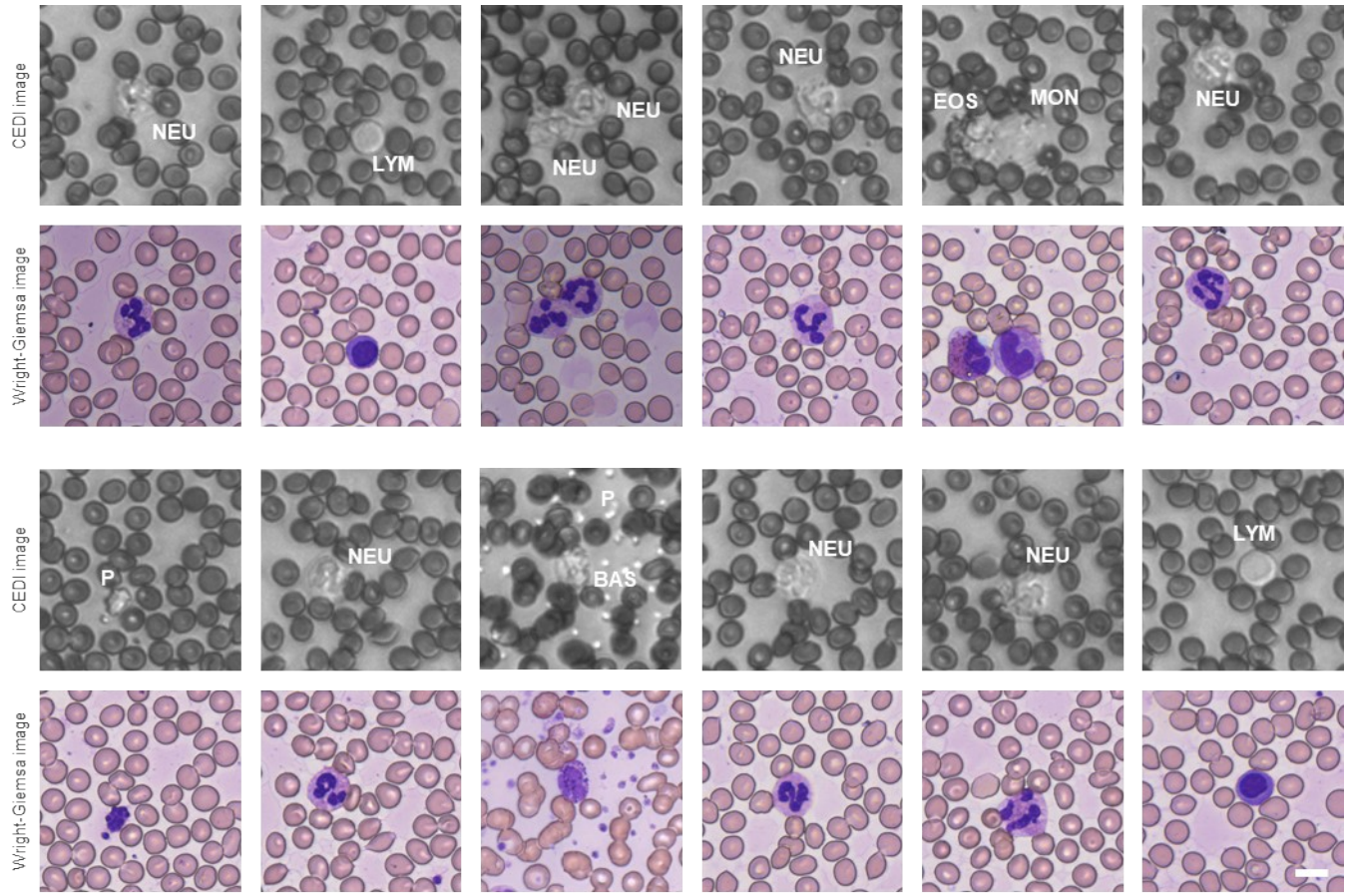


Fig. 8 Image pair of the CEDI images from the mobile blood analyzer and the Wright-Giemsa images from the conventional bright-field microscope (40X, 0.95 NA). The blood cell types for the cell presented in the image centers were marked. P: platelet, NEU: neutrophil, EOS: eosinophil, BAS: basophil, MON: monocyte, LYM: Lymphocyte. Scale bar: 10 μm.

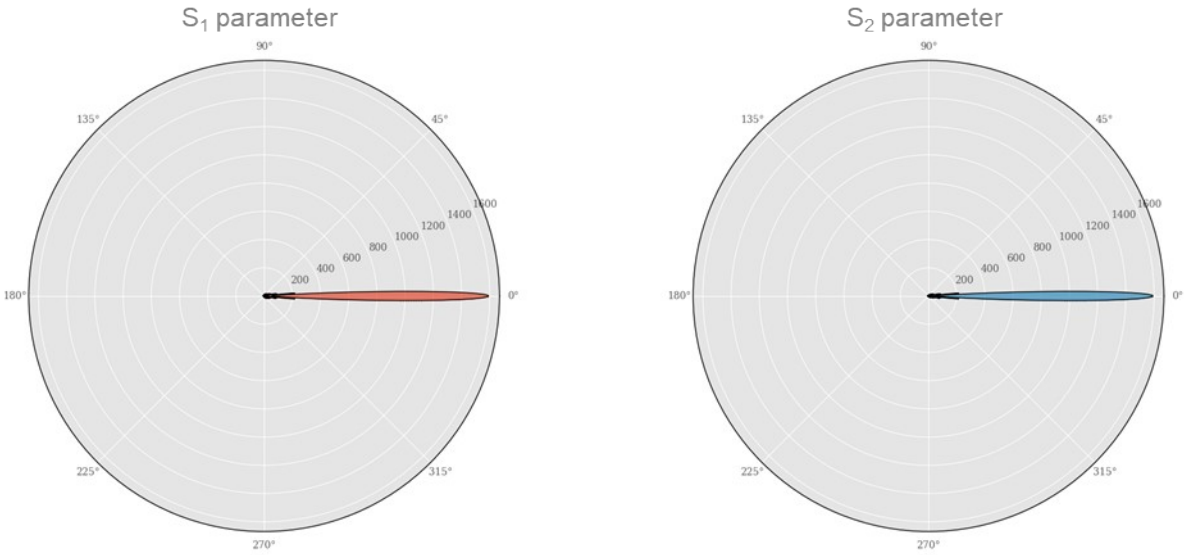


Fig. 9 Scattering amplitude maps $S_1$ (parallel to the scattering plane) and $S_2$ (perpendicular to the scattering plane) at scattering angle intervals of [0°， 360°] according to the Mie scattering theory. In the simulation, the light source is set as a plane wave with 0.415 μm light, the RBC diameter is set as 7.2 μm (the average RBC diameter for blood smears), the media refractive index is set as 1.0 (air refractive index); The RBC refractive index is calculated as[1]: $n = n_1 + in_2$. Here, $n_1$ and $n_2$, related to the hemoglobin concentration, are the real and imaginary parts of the complex refractive index, respectively. And $n_1 = n_0 + \alpha c$, $n_0$ presents the refractive index in the absence of hemoglobin and $\alpha$ presents the refractive index increment of hemoglobin under specific illumination wavelength $\lambda$, and $c$ presents the hemoglobin concentration; $n_2 = \frac{ln10\lambda\epsilon_{\mu M}c}{4\pi M}$, with $\epsilon_{\mu M}$ presents the micromolar extinction coefficient of the hemoglobin at wavelength $\lambda$, M presents the molar mass of hemoglobin. Under 0.415 μm light illumination, the $n_0$ approximates to 1.345 and $\alpha$ approximates to 0.0017 (dl/g) according to the study by O. Zhernovaya et al.[2]. Besides, the $\epsilon_{\mu M} = 363848x10^{-3}cm^2/\mu mol,\ M = 64500\ g/mol, c = 34\ g/dl$ (the normal pysical intraerythrocytic hemoglobin concentration[1]). According to the results, the scattering lights are highly concentrated within small forward-angle intervals, with up to 70% of $S_1$'s scattering energies lie in an angle interval of [-6.45°, 6.45°] and up to 70% of $S_2$'s scattering energies lie in an angle interval of [-11.56°, 11.56°]. Additionally, the reported miniature microscope's numerical aperture can achieve 0.25 from the resolution test results. The aperture angle of the miniature microscope is at least 14.5° [aperture angle = arcsin(0.25)]. Hence, the microscope can collect most of the scattering light of a single RBC. And the light attenuation when the lights go through a single RBC mainly contributes to light absorption rather than light scattering.

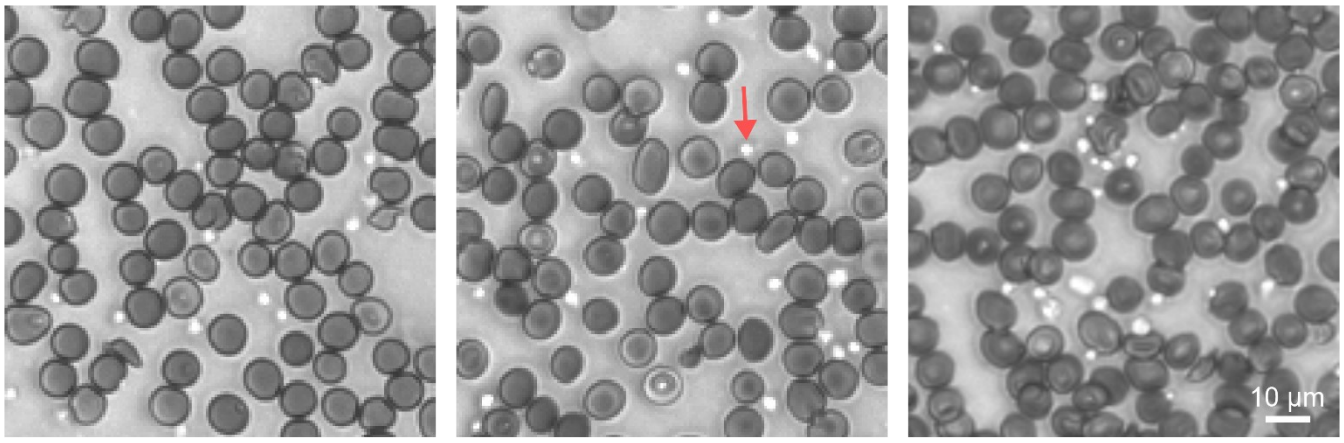


Fig. 10 CEDI images, captured by the miniature microscope, from a sample with increased platelet count. One of the platelet examples is indicated by the red arrow.

## Supplementary Tables

Table 1 Performance indexes for FWD testing.

| | Neutrophil | Eosinophil | Basophil | Lymphocyte | Monocyte | Average |
|---|---|---|---|---|---|---|
| Precision | 0.993 | 0.941 | 0.920 | 0.979 | 0.974 | 0.961 |
| Recall | 0.991 | 0.941 | 0.958 | 1.000 | 0.987 | 0.975 |
| F1 Score | 0.992 | 0.941 | 0.939 | 0.989 | 0.980 | 0.968 |

Table 2 Sample amount for FWD (n = 30)

| Sample | Image | Total WBC | Neutrophil | Eosinophil | Basophil | Lymphocyte | Monocyte |
|---|---|---|---|---|---|---|---|
| 1 | 145 | 326 | 273 | 1 | 8 | 28 | 16 |
| 2 | 150 | 242 | 133 | 5 | 2 | 91 | 11 |
| 3 | 160 | 207 | 109 | 60 | 1 | 34 | 3 |
| 4 | 178 | 341 | 287 | 2 | 1 | 43 | 9 |
| 5 | 87 | 118 | 78 | 4 | 0 | 25 | 10 |
| 6 | 164 | 245 | 133 | 2 | 3 | 82 | 25 |
| 7 | 118 | 848 | 825 | 1 | 1 | 12 | 9 |
| 8 | 189 | 290 | 202 | 5 | 1 | 65 | 17 |
| 9 | 174 | 293 | 159 | 4 | 2 | 108 | 20 |
| 10 | 149 | 237 | 167 | 1 | 0 | 65 | 4 |
| 11 | 141 | 210 | 130 | 2 | 0 | 75 | 3 |
| 12 | 147 | 189 | 122 | 2 | 2 | 61 | 2 |
| 13 | 163 | 263 | 178 | 2 | 1 | 79 | 3 |
| 14 | 180 | 290 | 244 | 9 | 2 | 27 | 8 |
| 15 | 89 | 191 | 92 | 10 | 1 | 73 | 15 |
| 16 | 119 | 328 | 180 | 10 | 5 | 67 | 66 |
| 17 | 85 | 184 | 144 | 0 | 0 | 34 | 6 |
| 18 | 131 | 235 | 196 | 1 | 2 | 34 | 2 |
| 19 | 68 | 104 | 75 | 14 | 0 | 12 | 1 |
| 20 | 94 | 190 | 135 | 3 | 0 | 44 | 8 |
| 21 | 154 | 258 | 101 | 11 | 2 | 143 | 2 |
| 22 | 30 | 187 | 181 | 0 | 0 | 3 | 2 |
| 23 | 45 | 330 | 323 | 0 | 0 | 3 | 4 |
| 24 | 50 | 343 | 335 | 1 | 0 | 3 | 4 |
| 25 | 90 | 184 | 155 | 1 | 2 | 23 | 5 |
| 26 | 50 | 92 | 79 | 1 | 1 | 11 | 1 |
| 27 | 90 | 147 | 120 | 6 | 1 | 14 | 6 |
| 28 | 100 | 166 | 137 | 7 | 1 | 18 | 4 |
| 29 | 70 | 152 | 129 | 0 | 6 | 10 | 7 |
| 30 | 90 | 202 | 174 | 1 | 4 | 16 | 7 |

Table 3 Statistics of the image gradient for the five WBC populations and the granulocyte.

| | Median | Interquartile Range | 95% Confidence Interval | |
|---|---|---|---|---|
| | | | Lower Limit | Upper Limit |
| Neutrophil | 121.513 | 21.213 | 118.680 | 133.800 |
| Eosinophil | 133.608 | 29.919 | 125.617 | 149.171 |
| Basophil | 106.214 | 18.540 | 103.043 | 114.253 |
| Lymphocyte | 81.885 | 13.192 | 77.739 | 86.032 |
| Monocyte | 134.037 | 21.810 | 125.968 | 142.106 |
| Granulocyte | 126.240 | 21.213 | 118.679 | 133.780 |

Table 4 Statistics of the image area for the lymphocyte, monocyte, and granulocyte.

| | Median | Interquartile Range | 95% Confidence Interval | |
|---|---|---|---|---|
| | | | Lower Limit | Upper Limit |
| Lymphocyte | 6391.450 | 1329 | 5782.540 | 7000.360 |
| Monocyte | 13778.700 | 1382 | 13034.410 | 14522.990 |
| Granulocyte | 10773.100 | 1584 | 10014.690 | 11531.510 |

Table 5 Statistics of the image mean intensity for the three granulocyte populations.

| | Median | Interquartile Range | 95% Confidence Interval | |
|---|---|---|---|---|
| | | | Lower Limit | Upper Limit |
| Neutrophil | 166.245 | 12.177 | 162.822 | 170.693 |
| Eosinophil | 150.308 | 10.721 | 144.177 | 152.438 |
| Basophil | 168.606 | 7.125 | 165.406 | 170.369 |

Table 6 Independence sample t-test for equality of image area, mean intensity, and gradient

| Image feature | | T-value | Degrees of freedom | P-value | Mean difference | Std. error difference | 95% Confidence interval of the difference | |
|---|---|---|---|---|---|---|---|---|
| | | | | | | | Lower | Upper |
| Image area | Gran Vs. Lym | 7.954 | 77 | $1.248x10^{-11}$ | 4225.821 | 531.291 | 3167.887 | 5283.756 |
| | Gran Vs. Mon | -5.810 | 77 | $1.335x10^{-7}$ | -3161.430 | 544.139 | -4244.950 | -2077.910 |
| | Lym Vs. Mon | -16.079 | 38 | $1.529x10^{-18}$ | -7387.250 | 459.448 | -8317.85 | -6457.150 |
| Image mean intensity | Eos Vs. Bas | -8.505 | 31.135 | $2.513x10^{-10}$ | -19.580 | 2.302 | -24.274 | -14.885 |
| | Eos Vs. Neu | 6.698 | 36.978 | $7.193x10^{-8}$ | 18.670 | 2.7887 | 13.023 | 24.319 |
| Image gradient | Lym Vs. Mon | -12.032 | 38 | $1.574x10^{-14}$ | -52.151 | 4.334 | -60.926 | -43.377 |
| | Bas Vs. Neu | 3.717 | 37 | $0.665x10^{-3}$ | 17.018 | 4.579 | 7.741 | 26.295 |

Table 7 Independence sample t-test for equality of RBC hemoglobin means (anemia versus health).

| T-value | Degrees of freedom | P-value | Mean difference | Std. error difference | 95% Confidence interval of the difference | |
|---|---|---|---|---|---|---|
| | | | | | Lower | Upper |
| -58.625 | 1259.401 | 0.000 | -11.289 | 0.193 | -11.667 | -10.911 |

Table 8 Independence sample t-test for equality of RBC area means (anemia versus health).

| T-value | Degrees of freedom | P-value | Mean difference | Std. error difference | 95% Confidence interval of the difference | |
|---|---|---|---|---|---|---|
| | | | | | Lower | Upper |
| -17.764 | | $9.996 \times 10^{-62}$ | -17.764 | -6.912 | -7.675 | -6.148 |

Table 9 Statistic data of the RBC hemoglobin and area for the anemia sample.

| | Median | Interquartile Range | 95% Confidence Interval | |
|---|---|---|---|---|
| | | | Lower | Upper |
| Hemoglobin | 21.509 | 5.370 | 21.269 | 21.913 |
| Area | 48.254 | 11.356 | 47.196 | 48.593 |

Table 10 Statistic data of the RBC hemoglobin and area for the health sample.

| | Median | Interquartile Range | 95% Confidence Interval | |
|---|---|---|---|---|
| | | | Lower | Upper |
| Hemoglobin | 33.064 | 4.813 | 32.683 | 33.078 |
| Area | 55.037 | 7.776 | 54.482 | 55.121 |

## References

1 J. Gienger, H. Groß, J. Neukammer and M. Bär, Determining the refractive index of human hemoglobin solutions by Kramers–Kronig relations with an improved absorption model, *Appl. Opt.*, 2016, **55**, 8951.
2 O. Zhernovaya, O. Sydoruk, V. Tuchin and A. Douplik, The refractive index of human hemoglobin in the visible range, *Phys. Med. Biol.*, 2011, **56**, 4013–4021.

 